Pergamon

Journal of Structural Geology, Vol. 19, No. 8, pp. 1111 to 1120, 1997

0191-8141/97 $17.00 + 0.00

PII: S0191-8141(97)00030-8

Magnetic fabrics and oblique ramp-related folding: A case study from the western Taurus (Turkey)

C. AUBOURG and D. FRIZON DE LAMOTTE

Université de Cergy-Pontoise, Département des Sciences de la Terre (CNRS URA 1759), 8 Le Campus, av. du Parc F95 011 Cergy-Pontoise cédex, France

A. POISSON

Université de Paris-Sud (Orsay), Laboratoire de Géologie Structurale (CNRS URA 1369), Bat. 504, F91 405 Orsay cédex, France

and

E. MERCIER

Université de Cergy-Pontoise, Département des Sciences de la Terre (CNRS URA 1759), 8 Le Campus, av. du Parc F95 011 Cergy-Pontoise cédex, France

(*Received* 9 *September* 1996; *accepted in revised form* 1 *March* 1997)

Abstract—An analysis of magnetic fabric has been performed in weakly deformed Paleocene–Eocene limestone adjacent to two subparallel ramp-related folds (Akseki and Ormana folds) from the western Taurus (Turkey). The magnetic fabric of tectonic origin records two trends of well-defined magnetic lineation: N160° ± 7° and N130° ± 14° in front of the Akseki and Ormana folds, respectively. The trend of the magnetic lineation is oblique to the Akseki fold, whereas in the Ormana fold, magnetic lineation and fold axis are subparallel. The observed change in the trend of magnetic lineation is probably linked to a change of the shortening direction that occurred during the development of the thrust system. This shows that the two subparallel folds result from two different translation vectors. © 1997 Elsevier Science Ltd.

INTRODUCTION

Similar to other deformation modes, the motion of thrust sheets is geometrically accommodated by rigid-body translation, rotation (folding and rotation about vertical axes) and strain (Ramsay and Huber, 1987). These three components occur universally and generally in combination. However, the relationships between these deformation components are not straightforward. It is possible to have far-travelled sheets with little strain or conversely sheets exhibiting significant strain that have not moved far (Elliott, 1976; Geiser, 1988; Mitra, 1994). The kinematic evolution of individual structures can be determined by linking finite-strain analysis with construction of balanced sections (Woodward *et al.*, 1986). In external fold-thrust structures, an initial strain resulting from layer-parallel shortening (LPS) occurs early because of pure shear that affects the whole sedimentary pile before folding (Engelder and Geiser, 1979; Geiser, 1988). Mitra (1994) has shown that in successive thrust sheets, LPS fabric was developed immediately before each sheet was emplaced. This chronological sequence gives us an efficient tool for discussing the kinematic compatibility between the LPS imprint and the subsequent folding. In particular, if folds are oblique to the main tectonic transport direction, the analysis of the LPS can give useful information about the 'true' shortening direction. In addition to the LPS, simple shear deformation occurs during the formation of ramp-related folds, but it is limited to the limbs (Suppe, 1985) and at the vicinity of the décollement levels as a consequence of shearing along these planes.

To study the kinematics of fault-related folds, anisotropy of magnetic susceptibility (AMS) is potentially a powerful approach. AMS is demonstrated to be an efficient tool to record subtle internal deformation resulting from pure shear (the layer-parallel shortening) (Averbuch *et al.*, 1992; Hirt *et al.*, 1995) or simple shear (Aubourg *et al.*, 1991). AMS reflects with great accuracy the preferred orientation of grains and/or crystal lattice of minerals that contribute to the magnetic susceptibility (Borradaile, 1988; Rochette *et al.*, 1992). The magnetic fabric derived from AMS measurements can be visualized as an ellipsoid with three principal axes ($K_1 > K_2 > K_3$). The clustering of K_1 and K_3 define, respectively, the magnetic lineation and the pole of the magnetic foliation. Common anisotropy parameters like $L = K_1/K_2$ and $F = K_2/K_3$ are used to describe the oblateness ($L < F$) or the prolateness ($L > F$) of the ellipsoid. From a compactional oblate fabric, characterized by a cluster of K_3 normal to bedding and K_1 axes scattered within bedding, the magnetic fabric is progressively modified according to the orientation of the

deformation axes. In compressional deformation, the first effect is a cluster of K_1 in a direction perpendicular to the shortening direction (Kligfield *et al.*, 1981; Kissel *et al.*, 1986; Lee *et al.*, 1990) whereas the cluster of K_3 remains normal to the bedding. Several studies by Kissel *et al.* (1986) show that these kinds of tectonic fabrics appear before any cleavage is expressed in the rocks. As the lineation defined by the cluster of K_1 is parallel to the incipient or expressed intersection between bedding and cleavage, it is frequently called 'intersection lineation' (Borradaile and Tarling, 1981). Therefore, even in the absence of tectonic microstructures, AMS may provide kinematic data that can be compared to mesostructures such as folds and faults.

This paper reports on AMS data obtained in front of two parallel ramp-related folds from the Akseki Taurus (Turkey). The geological implications of these results will be discussed.

GEOLOGICAL SETTING AND SAMPLING

The Akseki Taurus comprises two structural units (Monod, 1977) (Fig. 1a). The higher unit (Beyshir-Hadim

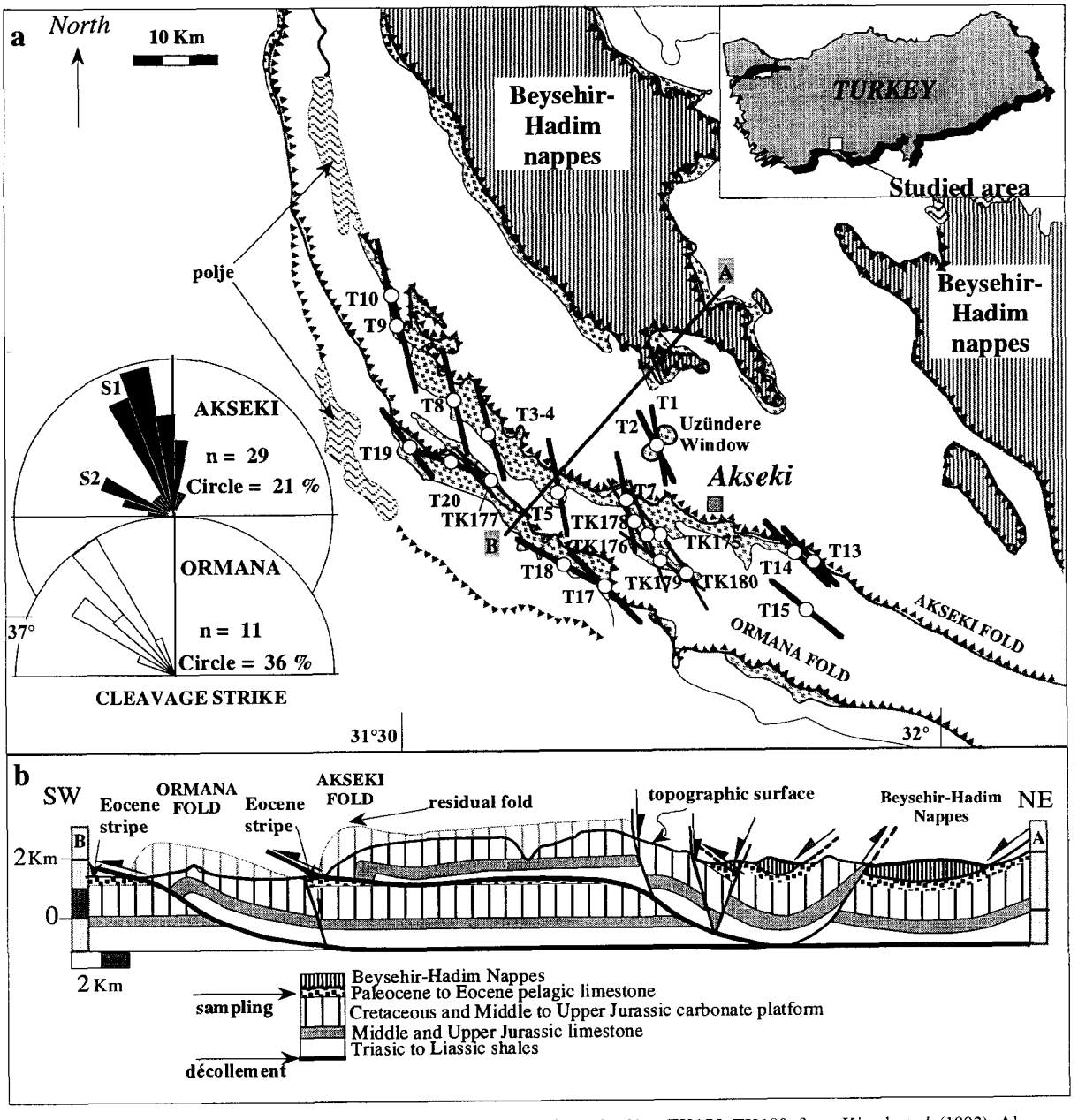

Fig. 1. (a) Schematic map of the studied area. Sites T1–T20, this study. Sites TK175–TK180, from Kissel *et al.* (1993). Also indicated are cleavage measurements in the Akseki and Ormana Eocene stripes and mean magnetic lineation after bedding correction (black lines). (b) General balanced cross-section through the studied area.

Nappe) forms a structurally complex association of ophiolitic rocks and sedimentary units of Palaeozoic and Mesozoic age. This ophiolitic nappe overlies the Akseki Thrust Belt. The latter comprises a thick carbonate platform of Jurassic–Cretaceous age. The transition between the platform and its substratum is expressed by Triassic detrital formations that form an important décollement level at regional scale. The carbonate platform supports a thin Paleocene–Eocene cover consisting of pelagic limestone ('scaglia' facies) in the external domain and of flysch in the internal domain in particular beneath the Beysehir-Hadim Nappe. The whole domain forms an arcuate fold-and-thrust belt in which the Akseki platform and the overlying Beysehir-Hadim Nappe are folded together.

In this paper we focus on the two major fold-thrust structures affecting the Akseki platform: the Akseki and the Ormana anticlines (Fig. 1b). These two folds are typical ramp-related folds and were emplaced following a piggy-back sequence, i.e. from NE to SW in present-day geographic coordinates (Monod, 1977). The Akseki and Ormana folds exhibit smooth trend changes from the north where they are oriented N–S to the south where they lie NW–SE. Geometrically they are asymmetric folds characterized by steep or overturned forelimbs resting on a subhorizontal décollement-fault (Fig. 1b). This upper flat is situated within the pelagic limestone of Eocene age. The Üzundere window situated behind the front of the Akseki anticline shows that a hangingwall sheet experienced a transport of at least 4 km. The geometry of the folds as well as some typical features, such as the existence of a residual fold between the forelimb and the horizontal long limb (Fig. 1b), leads us to interpret them as fault-propagation folds altered by a late transport on the upper flat (Jamison, 1987; Suppe and Medwedeff, 1990; Mercier *et al.*, 1997). According to the field data and geometrical modelling (see Discussion) the basal décollement (lower flat) is situated within the Triassic beds (Fig. 1b).

A previous palaeomagnetic study (Kissel *et al.*, 1993), based on 12 sites from the Cenozoic cover, gives evidence of a pre-folding characteristic magnetization that suggests a post-Eocene 45° clockwise rotation. This rotation that uniformly affects the whole Akseki Thrust Belt seems independent of folding and thrusting. Our sampling concerns the pink–yellow pelagic limestone of Eocene age, like the six sites sampled by Kissel *et al.* (1993) (TK175–TK180, Fig. 1a). We have sampled two sites in the Üzumdere window (T1 and T2), 10 sites (T3–T15) in the 'Akseki Eocene stripe' and four sites (T17–T20) in the 'Ormana Eocene stripe'. The Ormana and Akseki Eocene stripes form the direct footwall of the Ormana and Akseki folds, respectively (Fig. 1a). Therefore, these rocks did not suffer deformation due to bending over the ramps. Consequently, the recorded internal deformation could relate either to early LPS or to the shearing due to the rigid-body translation of the hangingwall of sheets on the upper flat. As shown in stereograms (Fig. 2), many sites do not exhibit any deformation markers or only spaced cleavage (sites T3, T4, T5, T8, T9, T10, T15, T19 and T20), and some show either a more developed cleavage (T7, T13, T17 and T18) or even two cleavages (T1, T2 and T14). In this latter case, the first cleavage is closer to a N–S strike than the second. The cleavage-bearing outcrops are mainly confined to or occur below the thrust faults. The rocks with two cleavages are strictly restricted to the Akseki Eocene stripe, particularly within the Üzundere window. The obliquity between bedding and cleavage where it exists (Fig. 2) suggests that it was the result of simple shear deformation. The attitude of the single cleavage varies accordingly to the geographic location: in the Akseki Eocene stripe, it is N–S to NNW–SSE whereas in the Ormana Eocene stripe it is NW–SE (Fig. 1a).

MAGNETIC FABRIC ANALYSIS

AMS measurements were performed using a Kappabridge susceptibility bridge KLY2 (Agico Ltd). The magnetic mineralogy of the sampled rocks has been described previously by Kissel *et al.* (1993). The main remanence carriers are magnetite, with a relatively small amount of haematite responsible for the red colour of the sediment. Paramagnetic clays are also present in various proportions and would contribute to the AMS. Statistics of AMS results performed using tensorial mean analysis (Jelinek, 1978) are compiled in Table 1. The mean susceptibility ($K_m = (K_1 + K_2 + K_3)/3$) measured from 146 specimens is ranging from -10^{-5} to 8×10^{-4} SI for calcite-rich and ferromagnetic-rich specimens, respectively. The shape of the AMS ellipsoid is generally oblate ($L = 1.02 \pm 0.02 < F = 1.06 \pm 0.04$) and locally prolate, in the Akseki Eocene stripe (Fig. 3). When plotting the degree of anisotropy $P = K_1/K_3$ vs the mean susceptibility K_m (Fig. 4), one can observe two trends:

(i) an enhancement of P up to 1.27 when magnetic susceptibility K_m is below 5×10^{-6} SI. Such an effect is an artefact due to the diamagnetic contribution (Rochette, 1987). A simple isotropic diamagnetic correction $K_i - \mathrm{DIA}$ ($i = 1, 2, 3$), with $\mathrm{DIA} = -14 \times 10^{-6}$ (Fig. 5), as proposed by Rochette (1987) is not completely satisfactory because a small relationship between P and K_m is still observed suggesting that the diamagnetic contribution is anisotropic;

(ii) a linear relationship between K_m and P for values of K_m between 50×10^{-6} and 400×10^{-6} SI. This suggests that the ferromagnetic contribution partly controls the high values of P (up to 1.15). According to Borradaile (1988), such a linear relationship between P and K_m rules out a possible calibration of deformation by using solely the AMS parameters. However, because there is no significant difference between the values of P from the Akseki and Ormana folds (Fig. 4), we can conclude that finite strain is of the same order in the two Eocene stripes.

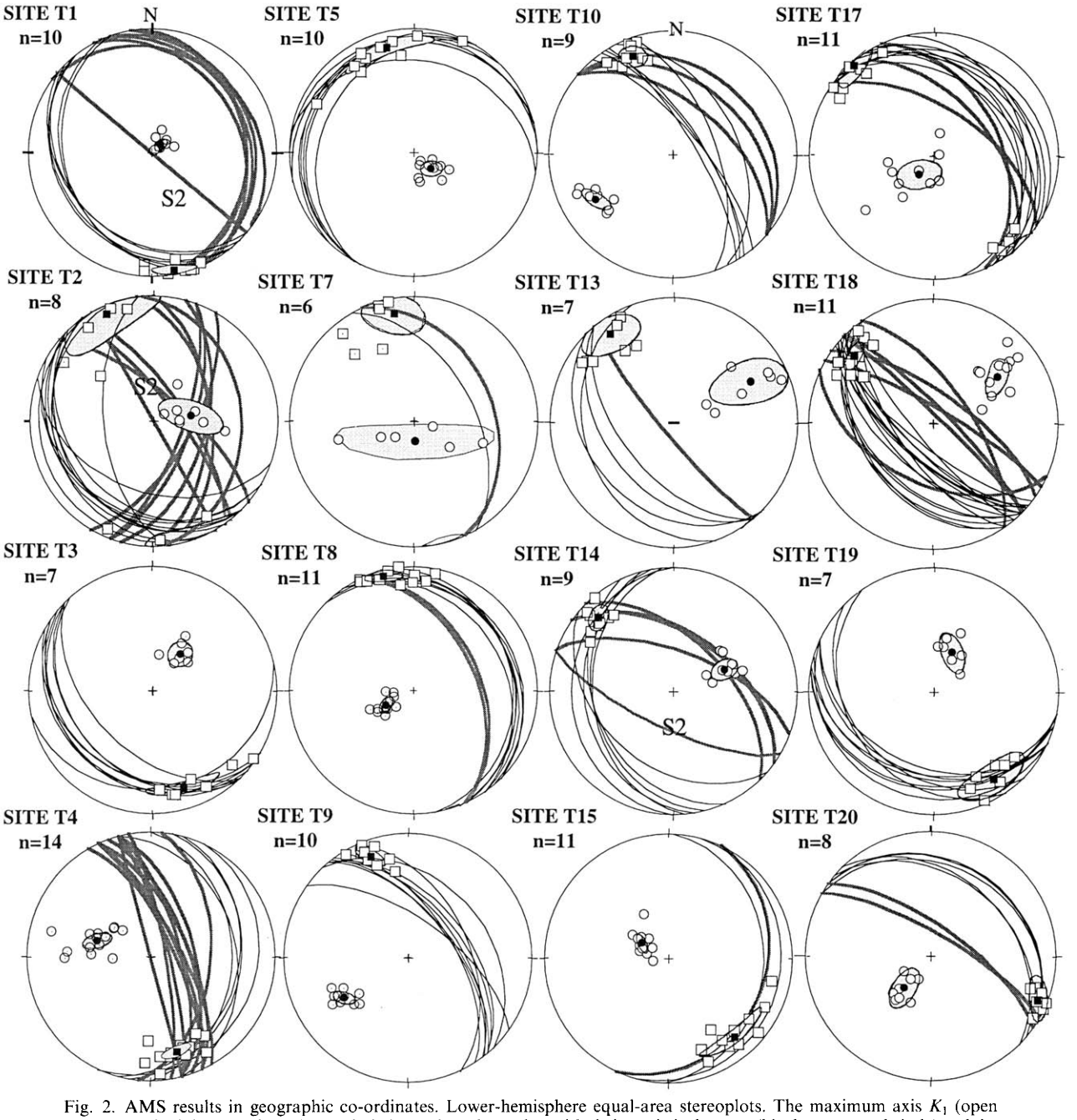

Fig. 2. AMS results in geographic co-ordinates. Lower-hemisphere equal-area stereoplots. The maximum axis K_1 (open squares) and minimum axis K_3 (open circles) are plotted together with their statistical means (black square and circle) and the ellipse of confidence at the 95% level. The bedding (black thin line) and the cleavage (shaded thick line) are also plotted.

Qualitatively, the grouping of the AMS axes is fairly good. The magnetic foliation (plane K_1–K_2) coincides well with bedding (Fig. 2). The magnetic lineation (grouping of K_1) is generally well defined with a half-confidence angle E_{12} (i.e. within the plane K_1–K_2) ranging from 8° (site T8) to 36° (site T5). The general trend of magnetic lineation after bedding correction is given in Table 1 and Fig. 6. AMS data from Kissel *et al.* (1993) (TK175–TK180) are shown also although the statistical processing is different. In their paper, they used a Fisher statistic that gives the same weight to all AMS data. We believe that the tensorial mean is more realistic because it is also sensitive to the intensity of anisotropy (Aubourg *et al.*, 1991). This would explain the small discrepancy in the trend of magnetic lineations. In the Ormana Eocene stripe, the average of the magnetic lineation (N130° ± 14°) is roughly parallel to the mean trend of the fold axis. When we examine in detail the Akseki Eocene stripe, we can see two trends: (i) the south-eastern sites (T13, T14, T15, TK180 and TK179) show a progressive change in the azimuth of K_1 from N130° to N150°; and (ii) the other sites display a constant azimuth

Table 1. $K_m=(K_1+K_2+K_3)/3$: mean susceptiblity (10^{-6} SI). $L=K_1/K_2$. $F=K_2/K_3$. D-K_i and I-K_i: declination and inclination of principal axes of magnetic susceptibility in geographic co-ordinates. E_{ij}: half-confidence angle within the plane K_iK_j. Standard deviation calculated at the 64% level is shown in parentheses

Site	n	K_m	L ($\times 10^{-3}$)	F ($\times 10^{-3}$)	D-K_1	I-K_1	D-K_3	I-K_3	E_{12}	E_{23}	E_{31}	Trend K_1
Eocene Akseki stripe												
T1	10	306 (73)	1.024 (5)	1.050 (23)	170	5	48	81	12	5	4	170±12
T2	8	31 (54)	1.014 (10)	1.038 (25)	336	7	81	65	29	15	8	154±29
T3	6	122 (74)	1.010 (9)	1.060 (30)	160	18	38	59	23	7	6	164±23
T4	14	295 (90)	1.040 (10)	1.070 (17)	165	22	286	53	9	10	4	156±9
T5	10	66 (67)	1.002 (2)	1.060 (27)	351	11	132	76	36	4	7	170±36
T7	6	308 (66)	1.020 (5)	1.100 (4)	350	13	175	76	20	56	14	170±20
T8	11	219 (49)	1.010 (8)	1.100 (22)	346	6	241	68	10	3	6	167±10
T9	10	273 (33)	1.010 (3)	1.070 (12)	340	15	237	39	11	5	8	167±11
T10	9	282 (71)	1.010 (6)	1.060 (21)	338	15	239	28	10	5	11	167±10
T13	7	104 (56)	1.020 (10)	1.050 (17)	318	11	56	35	20	32	15	133±20
T14	9	246 (45)	1.030 (8)	1.050 (20)	318	13	66	53	18	9	5	135±18
T15	11	118 (64)	1.010 (6)	1.050 (24)	143	18	299	71	19	6	3	141±19
TK175	10											142±6
TK176	8											162±8
TK178	8											150±9
TK179	7											120±18
TK180	10											150±8
Eocene Ormana stripe												
T17	11	91 (21)	1.020 (5)	1.040 (22)	316	2	220	74	12	15	9	136±12
T18	11	119 (87)	1.010 (10)	1.028 (28)	310	19	56	37	8	14	6	121±8
T19	7	160 (68)	1.020 (17)	1.080 (17)	153	13	22	65	21	16	11	145±21
T20	8	32 (9)	1.010 (3)	1.050 (8)	112	9	220	63	10	12	9	110±10
TK177	7											133±20

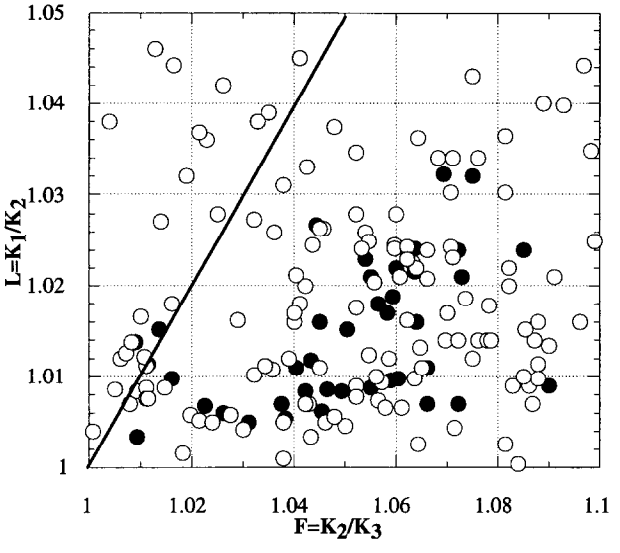

Fig. 3. Flinn-type diagram for magnetic fabric. Lineation L vs foliation F parameters. Open and close circles are P from the Akseki and Ormana Eocene stripes, respectively.

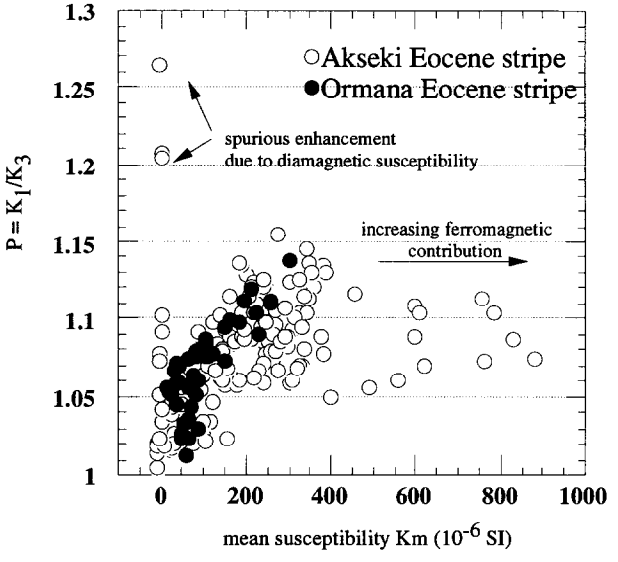

Fig. 4. Graph showing degree of anisotropy P vs mean susceptibility K_m. Open and close circles are P from the Akseki and Ormana Eocene stripes, respectively.

of N160° ± 7°. All are oblique to the anticline axis of the Akseki fold that exhibits a smooth curvature (Fig. 6) from N100° (site T13) to N160° (site T10).

DISCUSSION AND CONCLUSIONS

The origin of the observed magnetic lineation could be either sedimentary or tectonic. We reject a sedimentary origin for two main reasons: (1) some sites have experienced moderate deformation and, when the cleavage is expressed, the magnetic lineation is parallel to the intersection between bedding and cleavage (sites T1, T4, T14 and T18; Fig. 2); and (2) the magnetic lineation is different from the Akseki to the Ormana Eocene stripes but consistent within each area. Such behaviour can only

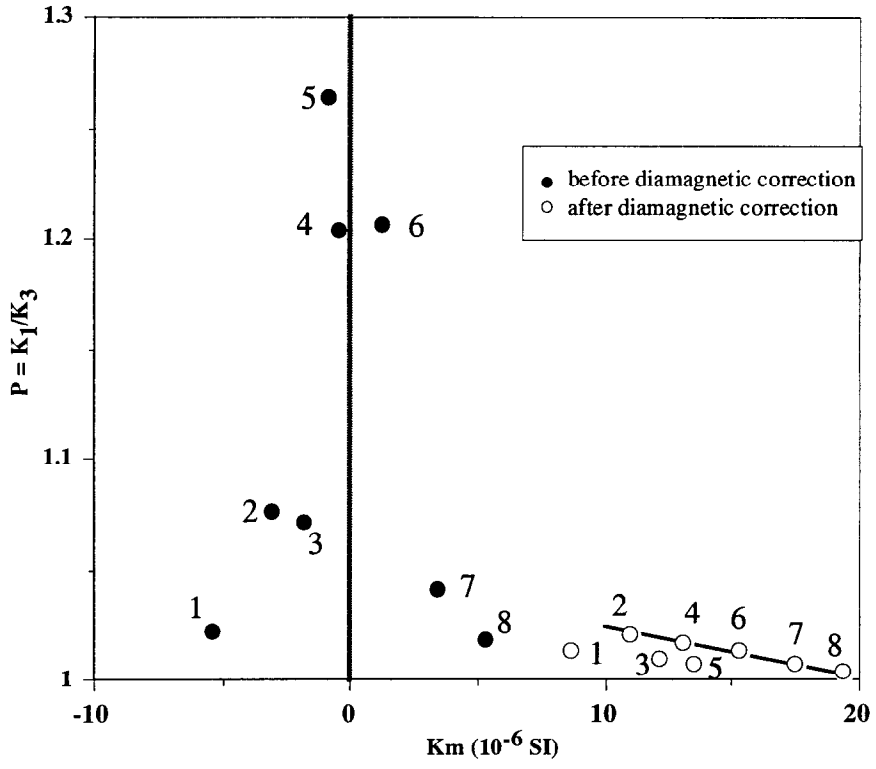

Fig. 5. Graph showing degree of anisotropy P vs mean susceptibility K_m for the site T3. Close circles correspond to bulk measurement, whereas open circles show the result after diamagnetic correction (K_i-(-14×10^{-6} SI); $i = 1, 2, 3$).

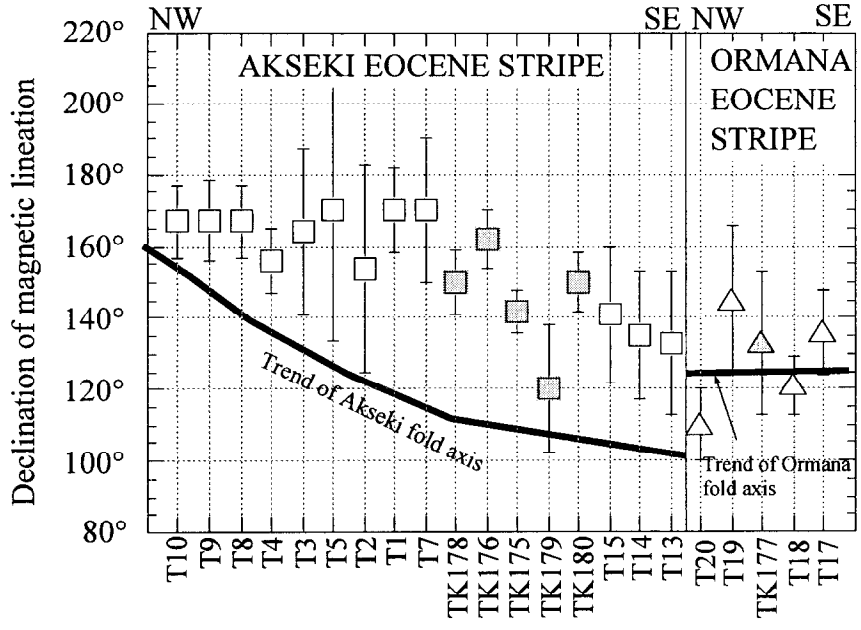

Fig. 6. Declination of mean K_1 after bedding correction with their confidence error (from Jelinek, 1978) vs location of the site relative to folds trend. Shaded symbols correspond to data from Kissel *et al.* (1993).

be explained with difficulty when using sedimentary processes. The magnetic lineation is expressed in all sites, in particular in those where cleavage is absent. This confirms that the magnetic fabric has the ability to record very low deformation in apparently undeformed rocks (Kissel *et al.*, 1986).

The cleavage that is oblique to bedding (Fig. 2) has a close spatial and geometric relationship to the thrust

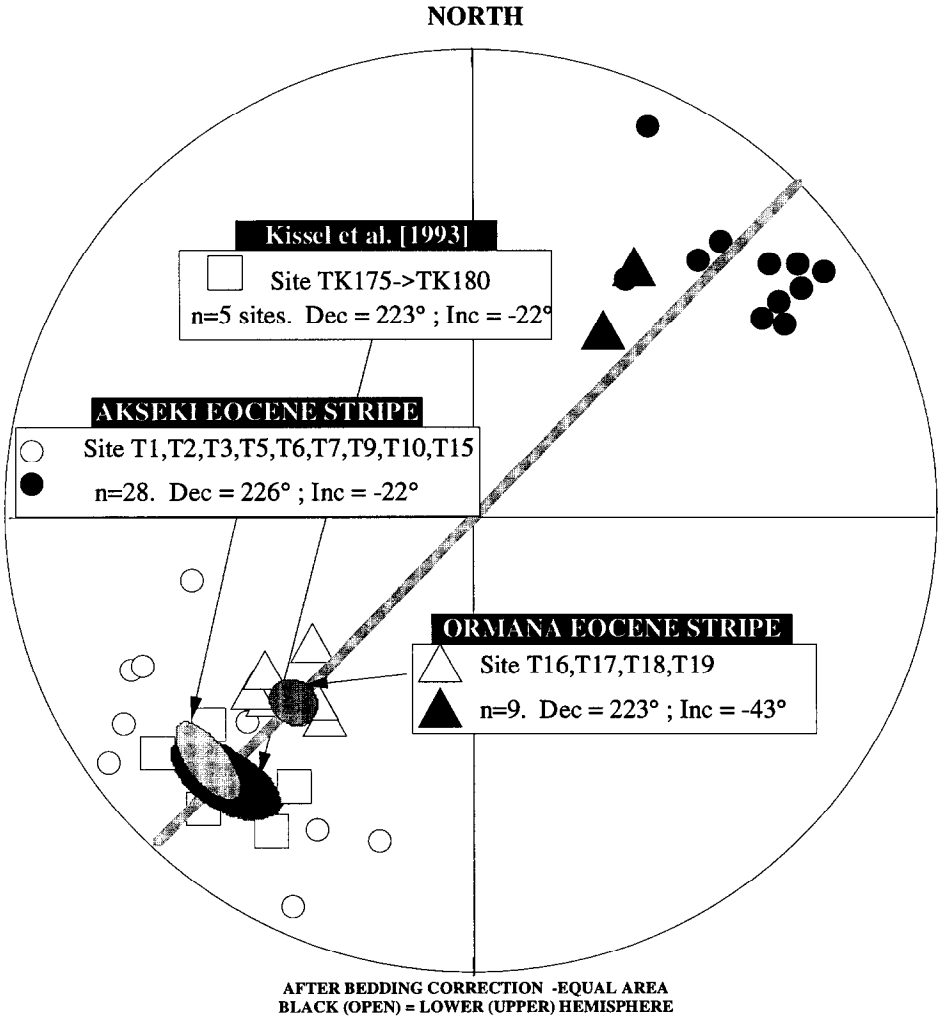

Fig. 7. Palaeomagnetic data after bedding correction from Kissel *et al.* (1993) and from our collection. All components were thermally demagnetized. A pre-folding characteristic magnetization has been isolated in the temperature range of 300–600°C.

faults, suggesting that it has been developed in relation to the displacement of the hangingwall sheets on their respective upper flats. In this context, two main hypotheses can be considered to explain the observed magnetic fabric. In the first hypothesis, the magnetic lineation could be taken to record the intersection lineation between bedding and the oblique expressed or incipient cleavage related to the shearing as mentioned above. This can be oberved in sites where cleavage is present (Fig. 2). It should be noted that magnetic lineation is parallel to the intersection between the first cleavage S_1 and the bedding despite the development of a second cleavage (sites T1 and T14, Fig. 2). Another hypothesis is to consider that the magnetic fabric records an earlier stage of LPS; in which case, the cleavage is developed without significant alteration of an inherited magnetic fabric. We favour the second hypothesis because the sites with no cleavage are relatively distant from the thrust planes and there is no microstructural evidence of internal deformation. Another fact that supports the latter hypothesis arises from the absence of 'transport lineation' parallel to the displacement, as observed in sediments gently deformed by simple shear (Aubourg *et al.*, 1991).

According to previous studies (Hrouda, 1991; Scheepers and Langereis, 1994) the magnetic lineation lies at right angles to the shortening direction (or its projection on the horizontal plane). The parallelism between the Ormana fold trend (Fig. 6) and the magnetic lineation (N130° ± 14°) in the Ormana Eocene stripe leads us to interpret the Ormana fold as a frontal fold. It implies that there is a close correspondence between fold-axis trend and magnetic fabric. In contrast, the obliquity of the magnetic lineation (N160° ± 7°) relative to the trend of the Akseki fold (Fig. 6) points out a discrepancy. Therefore, the Akseki fold appears to be oblique to the horizontal shortening that generated the magnetic fabric.

To explain these different trends of magnetic lineation and cleavage along the Akseki and Ormana Eocene stripes, two tectonic scenarios are possible:

(1) The variation records a differential rotation of about 30° between the two folds. As the thrust belt is

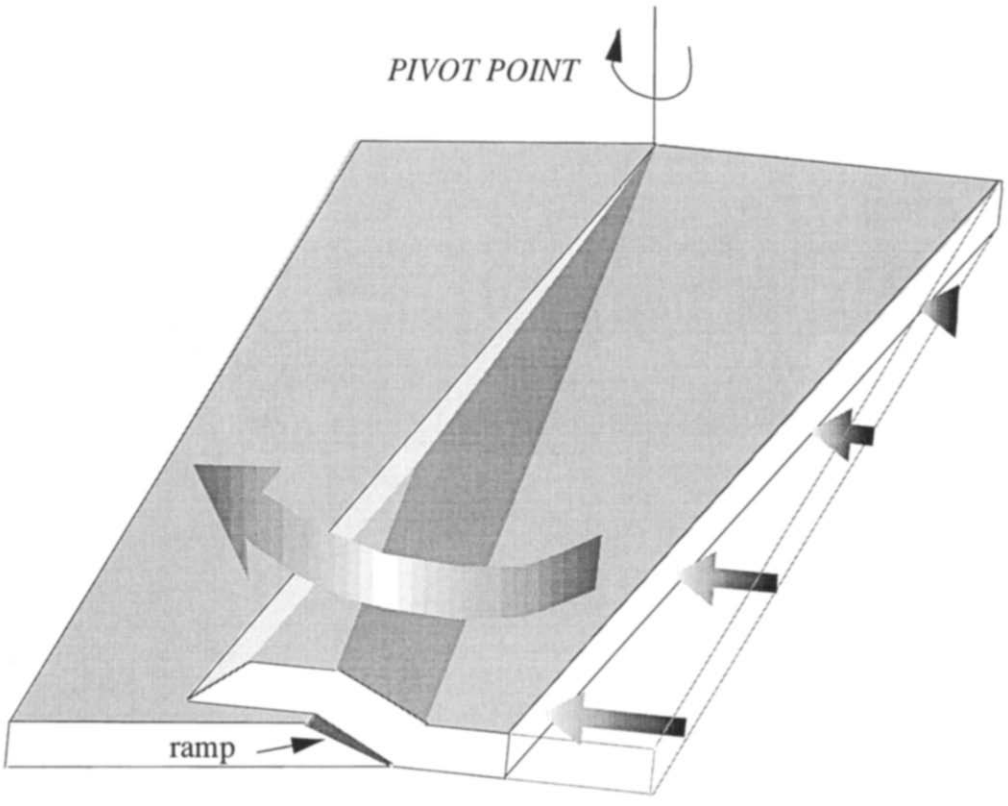

Fig. 8. Sketch diagram showing the geometry of a fold involving differential rotation about a vertical axis.

developed following a piggy-back sequence (Monod, 1977), the supposed rotation around a vertical axis should have occurred after the formation of the Akseki fold and during the formation of the Ormana fold. Additionally, the required horizontal decoupling zone on which the rotation must have acted was necessarily situated beneath the Ormana sheet and was propagating on the ramp related to the Ormana fold (Fig. 1b). Comparison of the paleomagnetic data from Kissel *et al.* (1993) with our preliminary data (Fig. 7) apparently shows the same pre-folding high-temperature component of magnetization within the two Eocene stripes. The bulk counterclockwise rotation about a vertical axis of 40–45° acts similarly in the two folds. Field and geometric evidence also rules out a 30° differential rotation of the two folds. On the one hand, we did not see any faults or microstructures that may indicate a rotation along the Ormana thrust. On the other hand, a 30° rotation of a block of about 50 km length with a pivot point at one extremity requires a differential displacement of some 25 km (Fig. 8). There is no evidence of an increase in the width of structural relief nor greater shortening that could be compatible with such differential displacement (Figs 1 & 8).

(2) The change in the orientation of magnetic lineation records a true change in the shortening direction (from N70° to N40°) that occurred between the building of the two ramp-related folds. Such a progressive modification of the shortening direction is supported by other evidence showing, at the orogen scale, a counterclockwise change in the path trajectory of the allochthonous sheets (Frizon de Lamotte *et al.*, 1995a). In addition, the second cleavage observed in sites T1, T2 and T14 (Fig. 2) also suggests an anticlockwise rotation of the shortening direction.

The preferred interpretation of the kinematic evolution of the Akseki and Ormana folds has been balanced and presented (Fig. 9) using the 'Rampe' (E.M.) software (Mercier *et al.*, 1997). The Akseki and Ormana folds are interpreted as being fault-propagation folds. As discussed in the introduction, it is worth noting that the AMS and cleavage data support that the deformation propagated progressively in the front of each individual fold. In this scenario, the Akseki fold is oblique with respect to the shortening direction.

It is now well known that in thrust systems the orientation of folds depends on the orientation of the folded planes and trend of the footwall ramps above which they develop, and is not directly linked to tectonic transport direction (Boyer and Elliott, 1982; Schirmer, 1988; Frizon de Lamotte *et al.*, 1995b). From this point of view, our study shows that the AMS method is an efficient tool for revealing the early stages of fold-thrust development, and so in determining the shortening direction independently from the orientation of fold

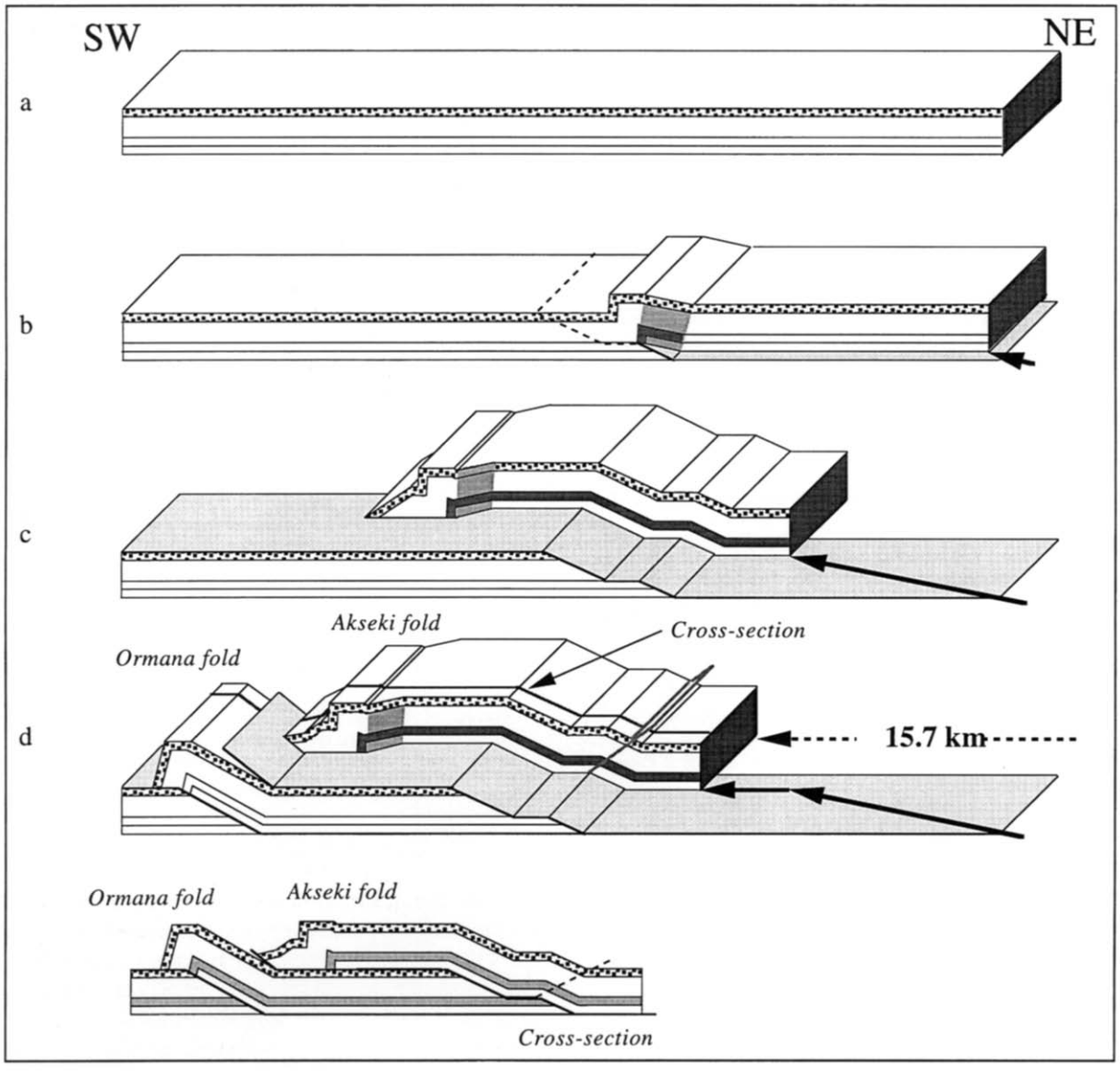

Fig. 9. Modelling of the Akseki and Ormana propagation fold-thrust structures using 'Rampe' (EM) software. To take into account the orientation of the magnetic lineation and the development of the cleavage, we consider that the change in the direction of the LPS occurred after the transport on the flat and before the formation of the Ormana fold. The final stage D is close to Fig. 1(b).

axes. Generally, interpretation problems will arise when a region has a complex pattern of folding and it is difficult to know whether the observed pattern results from superimposed events or from a unique or dominant tectonic transport direction. Our study illustrates the reverse case, where a very simple pattern of folding (Fig. 1) results from a complex displacement path (Fig. 9). This is an important consideration when constructing balanced cross-sections.

Acknowledgements—We greatly thank S. Brulé and A. S. Mériau who measured most of the samples. We also thank B. Henry and M. Le Goff (Geomagnetism Laboratory, Saint Maur) for allowing us to use the Kappabridge Kly-2 and other magnetic instruments. G. J. Borradaile and B. Van der Pluijm gave constructive criticism of the manuscript. We thank T. Andersen for improvements to the manuscript.

REFERENCES

Aubourg, C., Rochette, P. and Vialon, P. (1991) Subtle stretching lineation revealed by magnetic fabric of Callovian–Oxfordian black shales (French Alpes). *Tectonophysics* **185**, 211–223.

Averbuch, O., Frizon de Lamotte, D. and Kissel, C. (1992) Magnetic fabric as a structural indicator of the deformation path within a fold thrust structure: a test case from the Corbières (NE Pyrenees, France). *Journal of Structural Geology* **14**, 461–474.

Borradaile, G. (1988) Magnetic susceptibility, petrofabrics and strain. *Tectonophysics* **156**, 1–20.

Borradaile, G. and Tarling, D. H. (1981) The influence of deformation mechanisms on magnetic fabrics in weakly deformed rocks. *Tectonophysics* **77**, 151–168.

Boyer, S. E. and Elliott, D. E. (1982) Thrust systems. *Bulletin of the American Association of Petroleum Geologists* **66**, 1196–1230.

Elliott, D. (1976) The motion of thrust sheets. *Journal of Geophysical Research* **5**, 949–955.

Engelder, T. and Geiser, P. (1979) The relationship between pencil

cleavage and later parallel shortening within the Devonian section of the Appalachian Plateau. *Geology* **7**, 460–464.

Frizon de Lamotte, D., Poisson, A., Aubourg, C. and Temiz, H. (1995a) Chevauchements post-tortoniens vers l'ouest, puis vers le sud au coeur de l'angle d'Isparta (Taurus Turquie). Conséquences géodynamiques. *Bulletin de la Société géologique de France* **166**, 59–67.

Frizon de Lamotte, D., Guezou, J. C. and Averbuch, O. (1995b) Distinguishing lateral folds in thrust-systems; examples from Corbières (SW France) and Betic Cordilleras (SE Spain). *Journal of Structural Geology* **17**, 233–244.

Geiser, P. A. (1988) Mechanisms of thrust propagation: some examples and implications for the analysis of overthrust terranes. *Journal of Structural Geology* **10**, 829–845.

Hirt, A. M., Evans, K. F. and Engelder, T. (1995) Correlation between magnetic anisotropy and fabric for Devonian shales on the Appalachian plateau. *Tectonophysics* **247**, 121–132.

Hrouda, F. (1991) Models of magnetic anisotropy variations in sedimentary thrust sheets. *Tectonophysics* **185**, 203–210.

Jamison, W. R. (1987) Geometric analysis of fold development in overthrust terranes. *Journal of Structural Geology* **9**, 207–219.

Jelinek, V. (1978) Statistical processing of anisotropy of magnetic susceptibility mesured on group of specimen. *Studia Geophysica et geodinamica* **22**, 50–62.

Kissel, C., Averbuch, O., Frizon de Lamotte, D., Monod, O. and Allerton, S. (1993) First paleomagnetic evidence for a post-Eocene clockwise rotation of the Western Taurides thrust belt east of the Isparta reentrant (Southwestern Turkey). *Earth and Planetary Science Letters* **117**, 1–14.

Kissel, C., Barrier, E., Laj, C. and Lee, T. Q. (1986) Magnetic fabric in underformed marine clays from compressional zones. *Tectonics* **5**, 769–781.

Kligfield, R., Owens, W. H. and Lowrie, W. (1981) Magnetic susceptibility anisotropy, strain, and progressive deformation in Permian sediments from the Maritime Alps (France). *Earth and Planetary Science Letters* **55**, 181–189.

Lee, T.-Q., Kissel, C., Laj, C., Chorn-Shern, H. and Yi-Teh, L. (1990) Magnetic fabric analysis of the Plio-Pleistocene sedimentary formations of the coastal range of Taiwan. *Earth and Planetary Science Letters* **98**, 23–32.

Mercier, E., Outtani, F. and Frizon de Lamotte, D. (1997) Late-stage evolution of fault propagation folds: principles and example. *Journal of Structural Geology* **19**, 185–193.

Mitra, G. (1994) Strain variation in thrust sheets across the Sevier fold-and-thrust belt (Idaho–Utah–Wyoming): implications for section restoration and wedge taper evolution. *Journal of Structural Geology* **16**, 585–602.

Monod, O. (1977) Recherches géologiques dans le Taurus occidental au Sud de Beysehir (Turquie). Ph.D. thesis, Université de Paris-Sud.

Ramsay, J. G. and Huber, M. I. (1987) *Modern Structural Geology, Vol. 2: Folds and Fractures*. Academic Press, London.

Rochette, P. (1987) Magnetic susceptibility of the rock matrix related to magnetic fabric studies. *Journal of Structural Geology* **9**, 1015–1020.

Rochette, P., Jackson, J. and Aubourg, C. (1992) Rock magnetism and the interpretation of ansisotropy of magnetic susceptibility. *Review of Geophysics* **30**, 209–226.

Scheepers, P. J. J. and Langereis, C. G. (1994) Magnetic fabric of Pleistocene clays from the Tyrrhenian arc: A magnetic lineation induced in the final stage of the middle Pleistocene compressive event. *Tectonics* **13**, 1190–1200.

Schirmer, T. W. (1988) Structural analysis using thrust-fault hanging-wall sequence diagrams: Ogden duplex, Wasatch Range, Utah. *Bulletin of the American Association of Petroleum Geologists* **72**, 573–585.

Suppe, J. (1985) *Principles of Structural Geology*. Prentice-Hall, Englewood Cliffs, New Jersey.

Suppe, J. and Medwedeff, D. A. (1990) Geometry and kinematics of fault-propagation folding. *Eclogae Geologicae Helvetiae* **83**, 409–454.

Woodward, N. B., Gray, D. R. and Spears, D. B. (1986) Including strain data in balanced cross-sections. *Journal of Structural Geology* **8**, 313–324.